

# AdaptiveK Sparse Autoencoders: Dynamic Sparsity Allocation for Interpretable LLM Representations

Yifei Yao

Zhejiang University  
yifei3.23@intl.zju.edu.cn

Mengnan Du

New Jersey Institute of Technology  
mengnan.du@njit.edu

## Abstract

Understanding the internal representations of large language models (LLMs) remains a central challenge for interpretability research. Sparse autoencoders (SAEs) offer a promising solution by decomposing activations into interpretable features, but existing approaches rely on fixed sparsity constraints that fail to account for input complexity. We propose **Adaptive Top K Sparse Autoencoders (AdaptiveK)**, a novel framework that dynamically adjusts sparsity levels based on the semantic complexity of each input. Leveraging linear probes, we demonstrate that context complexity is linearly encoded in LLM representations, and we use this signal to guide feature allocation during training. Experiments across three language models (Pythia-70M, Pythia-160M, and Gemma-2-2B) demonstrate that this complexity-driven adaptation significantly outperforms fixed-sparsity approaches on reconstruction fidelity, explained variance, and cosine similarity metrics while eliminating the computational burden of extensive hyperparameter tuning.

## 1 Introduction

As large language models (LLMs) continue to advance, understanding their internal representations becomes increasingly crucial yet challenging. These models operate as “black boxes” with activation spaces that resist straightforward analysis [1, 2]. Individual components typically respond to multiple unrelated concepts (polysemanticity) [3], while the models encode more distinct features than their dimensional capacity would suggest (superposition) [4, 5, 6]. This efficient but complex encoding creates a significant interpretability barrier as traditional approaches cannot untangle the overlapping information patterns. Sparse autoencoders (SAEs) [7, 8] address this challenge by decomposing model activations into sparse combinations of interpretable features, revealing the underlying structure of the model’s representations.

Recent research has rapidly expanded the capabilities of sparse autoencoders, scaling them to extract millions of interpretable features from frontier models [9] while introducing numerous architectural innovations [10, 11, 12, 13, 14, 15, 16, 17, 18, 19]. However, despite these advancements, current SAE architectures rely on uniform sparsity constraints regardless of input complexity. Whether through activation-limiting approaches like TopK [11] and BatchTopK [12] that enforce a fixed number of active features ( $k$ ), or penalty-based methods like Gated SAEs [10] and P-anneal [17] that apply consistent regularization pressure, these designs create fundamental inefficiencies where conceptually simple inputs receive excessive representational capacity while complex inputs face insufficient feature allocation. This limitation becomes increasingly problematic at scale as Gao et al. [11] demonstrate that larger language models require proportionally more features to achieve comparable reconstruction quality. Moreover, finding optimal sparsity settings requires extensive hyperparameter experimentation to navigate the critical reconstruction-sparsity trade-off [20].

To overcome this limitation, we propose that *a sparse autoencoder should adaptively adjust sparsity levels based on input complexity*. When a simple semantic concept can be effectively explained and

reconstructed using only a few features, activating additional features becomes unnecessary. This approach not only conserves computational resources but also prevents unnecessary feature activation on simpler texts, reducing both overfitting and representational noise.

How can we define semantic simplicity or complexity within LLM representation spaces? Peters et al. [21] demonstrated that probes can map LLM intermediate representations to semantic and syntactic information. Similarly, higher-level concepts such as political perspective [22], sentiment [23], and spatiotemporal information [24] have been shown to be linearly represented in activation spaces. Based on these observations, we hypothesize that the internal representations formed by large language models during text processing naturally encode multidimensional properties of text, including its complexity.

Our study first establishes that text complexity is linearly encoded in language model representations. We score contexts using GPT-4.1-mini API [25] across six semantic dimensions to create aggregate complexity scores, then train linear regression probes on model activations to predict these scores. Experiments with three different scale LLMs demonstrate high correlation coefficient, confirming our hypothesis that LLMs naturally encode text complexity in their representation spaces. Analysis reveals that texts of varying complexity require proportional representational capacity, with complex inputs necessitating more active features for accurate encoding. This key insight suggests that adaptive sparsity mechanisms could significantly improve autoencoder efficiency.

Based on our complexity prediction capabilities, we develop the **Adaptive Top K Sparse Autoencoder (AdaptiveK SAE)**, which to our knowledge is the first work to solve computational efficiency bottlenecks in sparse autoencoder training while maintaining feature quality. Our approach first quantifies the inherent complexity of each context using a linear probe trained on multi-dimensional complexity annotations. This complexity score then determines an appropriate sparsity level, allowing more features to activate for complex inputs while maintaining high sparsity for simpler ones. This complexity-driven adaptation achieves an improved balance between reconstruction quality, sparsity, and interpretability. Experiments demonstrate that our framework outperforms fixed-sparsity approaches across multiple model scales. Our main contributions can be summarized as follows:

- We propose AdaptiveK Sparse Autoencoders, a novel framework that dynamically adjusts sparsity levels based on input complexity.
- We demonstrate that text complexity is linearly encoded in model representations, establishing a direct relationship between semantic complexity and representational capacity needs in LLMs.
- Experiments across three LLMs show that our SAE consistently outperforms fixed-sparsity baselines on reconstruction fidelity, explained variance, cosine similarity and other metrics.

## 2 Preliminaries and Motivation

### 2.1 Baseline Sparse Autoencoder

Following the initial works that introduced SAEs for decomposing model representations [8], a variety of architectural refinements have emerged. Our comparative analysis of these baselines was facilitated by the dictionary\_learning library [26]. Foundational ReLU SAEs [7] and the refined one [27] typically map an input activation  $x \in \mathbb{R}^d$  to a sparse latent  $z \in \mathbb{R}^M$  (where  $M \gg d$ ) and then to a reconstruction  $\hat{x}$ . The core operations involve an encoder:

$$z = \text{ReLU}(W_{enc}(x - b_{pre}) + b_{enc}), \quad (1)$$

and a decoder:

$$\hat{x} = W_{dec}z + b_{pre}, \quad (2)$$

with a training loss that combines reconstruction error with an  $L_1$  sparsity penalty on  $z$ .

$$L = \|x - \hat{x}\|_2^2 + \lambda \|z\|_1. \quad (3)$$

To mitigate issues like feature shrinkage from the  $L_1$  penalty, Gated SAEs [10] decouple the  $L_1$ -penalized feature selection gate  $g(x)$  from magnitude estimation  $m(x)$ , forming activations as  $z = g(x) \odot m(x)$ . Other approaches enforce sparsity directly: TopK SAEs [11] select the K highest pre-activations.

$$z = \text{ReLU}(\text{ReLU}(W_{enc}(x - b_{pre}) + b_{enc}), K). \quad (4)$$

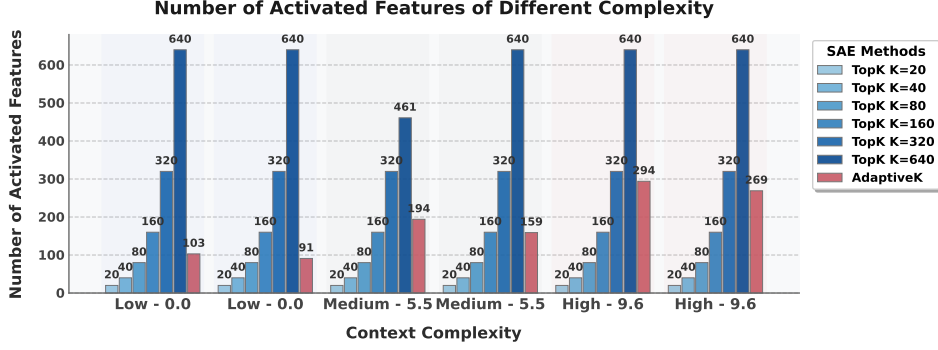


Figure 1: Two samples were selected from each complexity level (simplest=0, moderate=5.5, and most complex=9.6) from test set. In TopK SAE, feature activation strictly follows the k value between 20-320, but often falls below the threshold when k=640. For Pythia-160M, fixed TopK SAEs (blue) maintain constant activation, while AdaptiveK (red) dynamically scales with context complexity.

BatchTopK SAEs [12] extend this by selecting the top  $N \times K$  activations across a batch of  $N$  samples. JumpReLU SAEs [13] utilize a discontinuous activation  $z_i = \text{act}_i \cdot H(\text{act}_i - \theta_i)$  with a learned threshold  $\theta_i$  (where  $\text{act}_i$  is preactivation and  $H$  is Heaviside), often paired with a  $L_0$  sparsity term and trained via Straight-Through Estimators. For refining loss-based sparsity, P-anneal ReLU SAEs [17] employ an  $L_p$  norm penalty,  $\lambda \sum_i |z_i|^p$ , where  $p$  anneals from 1 towards 0. Lastly, to address feature hierarchy and issues like splitting or absorption, Matryoshka BatchTopK SAEs [16] train nested dictionaries of increasing capacity, using BatchTopK for sparsity within each level.

## 2.2 Our Motivation

Despite advances in SAE scalability and architecture, current approaches face a fundamental limitation: they apply uniform sparsity constraints regardless of input complexity. This “one-size-fits-all” approach creates inefficiencies across the representation space. Whether employing fixed activation methods such as TopK [11] or regularization techniques like Gated SAEs [10] existing architectures cannot adapt to the varying complexity demands of different inputs. As shown in Figure 1 conventional SAE methods with fixed K maintain constant activation (e.g., 80 features across all complexities), while our AdaptiveK dynamically scales from 103 to 394 features based on input complexity. This inefficiency becomes more pronounced at scale, determining optimal sparsity parameters necessitates extensive hyperparameter optimization to balance reconstruction fidelity against sparsity constraints.

Our approach is motivated by the observation that text complexity is linearly encoded in language model representations, suggesting a more efficient solution: adaptively adjusting sparsity levels based on input complexity. Simple inputs require fewer features for reconstruction, while complex ones need more representational capacity. This adaptive allocation improves computational efficiency, reduces overfitting on simple inputs, and enhances interpretability, all achieved within a single training run without extensive hyperparameter tuning.

## 3 The Proposed AdaptiveK Sparse Autoencoder

In this work, we propose AdaptiveK Sparse Autoencoder that dynamically adjusts sparsity constraints according to input complexity. Our AdaptiveK Sparse Autoencoder addresses the fundamental inefficiency of uniform sparsity constraints by allocating representational capacity proportionally to content complexity (see Figure 2). Specifically, the AdaptiveK SAE consists of two primary components: (1) a linear probe that predicts input complexity (Section 3.1), and (2) the sparse autoencoder with AdaptiveK activation (Section 3.2). Additionally, we introduce our three-phase scheme for effective training of our proposed AdaptiveK SAE (Section 3.3).

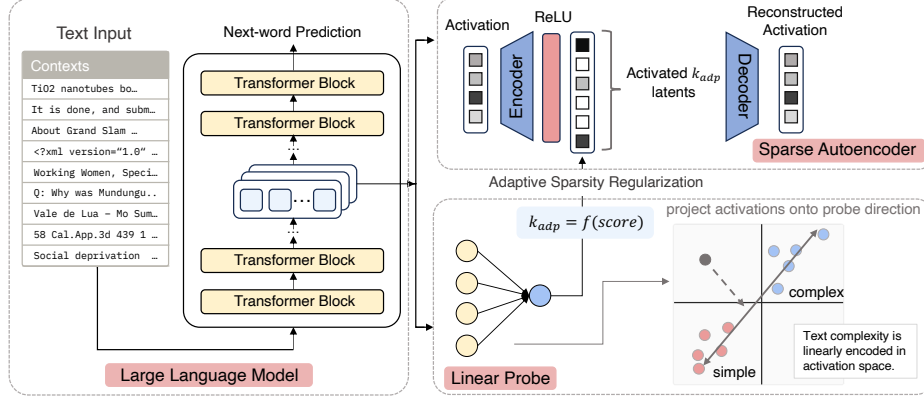


Figure 2: Overall pipeline of the AdaptiveK SAE framework. The text input is fed into a LLM to extract internal activations, which are then passed through both a linear probe that predicts text complexity and a SAE for decomposition. During the training process of the SAE, the linear probe’s complexity score dynamically determines the number of features to activate, allowing more features for complex inputs and fewer for simple ones.

### 3.1 Training Linear Probes to Predict Context Complexity

#### 3.1.1 Linear Probe for Complexity Prediction

Our dataset comprises contexts from pile-uncopyrighted [28], each containing 1024 tokens. Complexity is quantified on a scale from 0 to 10, based on a six-dimensional evaluation (lexical complexity, syntactic complexity, conceptual density, domain specificity, logical structure and logical structure) by GPT-4.1-mini (scoring prompts detailed in Appendix A), yielding target labels  $y_i$ . These complexity scores are floating-point numbers with one decimal place. For each context, we extract the hidden state activations of the last token from selected layers of the auto-regressive transformer language models Pythia-70M, Pythia-160M [29] and Gemma-2-2B [30], which encapsulate contextual information. The input data for each context  $i$  is represented as a pair  $[x_i, y_i]$ , where  $x_i \in \mathbb{R}^{d_{\text{model}}}$  is the vector of hidden state activations and  $y_i \in \mathbb{R}$  is the corresponding complexity score.

Following Gurnee and Tegmark [24], we employ ridge regression to mitigate overfitting and multicollinearity issues common with high-dimensional activation vectors [22]. The objective is to find the weight vector  $w \in \mathbb{R}^{d_{\text{model}}}$  and bias term  $b \in \mathbb{R}$  that minimize the  $L_2$ -regularized squared loss:

$$L(w, b) = \frac{1}{n} \sum_{i=1}^n (y_i - (w^T x_i + b))^2 + \frac{\lambda}{2} \|w\|_2^2, \quad (5)$$

where  $n$  is the number of training contexts, and  $\lambda$  is the regularization hyperparameter. The activation matrix  $A \in \mathbb{R}^{n \times d_{\text{model}}}$  is constructed by concatenating these feature vectors, with the target vector defined as  $y \in \mathbb{R}^n$ . With implicit bias handling (e.g., by centering the data or adding a feature column of ones to  $A$ ), the optimal weight vector  $\hat{w}$  is given by the closed-form solution [31]:

$$\hat{w} = (A^T A + \lambda I)^{-1} A^T y. \quad (6)$$

To determine the optimal regularization strength  $\lambda$ , we perform 5-fold cross-validation. For each  $\lambda$  in the set  $\{0.001, 0.01, 0.1, 1.0, 10.0, 100.0, 1000.0\}$ , the probe is trained on four folds and evaluated on the held-out fold using the root mean squared error (RMSE). We select  $\lambda = 100.0$ , which yields the lowest average RMSE across the folds. The final probe, with parameters  $(\hat{w}, \hat{b})$ , is then trained on the entire dataset using this optimal  $\lambda$ . Subsequently, this trained probe is used to predict complexity scores for new contexts based on their last token activation  $x$  via the linear function  $\hat{y} = \hat{w}^T x + \hat{b}$ . More training details will be presented in Appendix A.

#### 3.1.2 Evaluating the Linear Representation Hypothesis

As will be mentioned in Section 5.2, a growing number of high-level features have been demonstrated to exist linearly in LLM representation spaces. However, context complexity is indeed a multifaceted

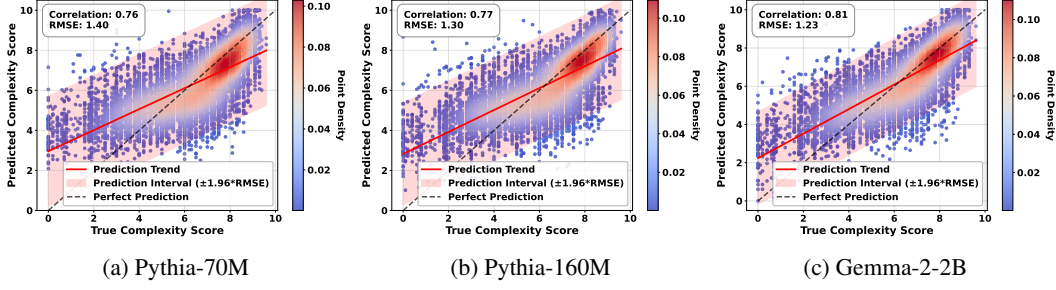


Figure 3: Visualization of linear probe performance across three LLM scales. Points represent test contexts, with redder areas indicating higher sample density. The red line depicts predicted complexity trends. The red line depicts predicted complexity trends. Most samples fall within prediction intervals, confirming the linear probe’s effectiveness. Spearman Correlation and RMSE values (upper left) demonstrate improved prediction accuracy with increasing model scale.

construct: it spans multiple linguistic dimensions, including lexical, syntactic complexity, etc., so it differs fundamentally from the single-attribute features investigated in previous work.

By comparing the performance of linear probes, MLP, and XGBoost in predicting context complexity, we provide evidence for the linear encoding of context complexity features in language model representation spaces. We contrasted a single-hidden-layer MLP with the structure  $f(\mathbf{x}) = \mathbf{W}_2 \text{ReLU}(\mathbf{W}_1 \mathbf{x} + \mathbf{b}_1) + \mathbf{b}_2$  containing 256 neurons in the hidden layer, and an XGBoost model that minimizes error through gradient boosting across multiple decision trees, with the prediction formula  $\hat{y}_i = \sum_{k=1}^K f_k(\mathbf{x}_i)$ , against our linear regression probe.

As shown in Table 1, linear model is comparable to theoretically more expressive nonlinear models like XGBoost across all three metrics: Pearson correlation coefficient, Spearman correlation coefficient, and RMSE. These findings extend the applicability of the linear representation hypothesis to multifaceted features such as context complexity. Figure 3 visualizes our probe’s performance on test data across three models. Each point represents one context from the test set, showing the predicted versus true complexity score. With most points falling within the prediction interval ( $\pm 1.96 \times \text{RMSE}$ ), this performance confirms that context complexity is largely encoded linearly in representation space.

Table 1: Comparison of Linear Probe, MLP, and XGBoost models for context complexity prediction on Pythia-70M, trained on 250,000 contexts and evaluated on 10,000 test samples using RMSE, Pearson, and Spearman metrics.

Probe	RMSE	Pearson	Spearman
Linear	1.41	0.72	0.76
MLP	1.37	0.74	0.77
XGBoost	1.42	0.71	0.74

### 3.2 AdaptiveK Sparse Autoencoder Architecture

Unlike existing SAEs apply uniform sparsity constraints across all inputs, requiring extensive hyperparameter experimentation, our AdaptiveK Sparse Autoencoder incorporates a complexity estimation component that adaptively determines the appropriate sparsity level for each context. The overall pipeline is shown in Figure 2.

For an input activation vector  $x \in \mathbb{R}^d$ , we first use the linear probe described in Section 3.1 to compute a complexity score  $c$ :  $c = \hat{w}^T x + \hat{b}$ , where  $\hat{w} \in \mathbb{R}^d$  and  $\hat{b} \in \mathbb{R}$  are trained from the ridge regression. This complexity score is then mapped to a sparsity level  $k_{\text{adp}}$  through a sigmoid-based transformation:

$$k_{\text{adp}} = k_{\min} + \frac{1}{1 + e^{-s \cdot \left( \frac{c - c_{\min}}{c_{\max} - c_{\min}} - 0.5 \right)}} \cdot (k_{\max} - k_{\min}), \quad (7)$$

where  $k_{\min}$  and  $k_{\max}$  define the range of possible  $k_{\text{adp}}$  values,  $c_{\min}$  and  $c_{\max}$  represent the minimum and maximum complexity scores, and  $s$  controls the steepness of the sigmoid function. The sparse autoencoder component then processes the input with an adaptive TopK activation function:

$$z = \text{TopK}(W_{\text{enc}}(x - b_{\text{pre}}), k_{\text{adp}}), \quad (8)$$

where  $\text{TopK}(\cdot, k_{\text{adp}})$  retains only the  $k_{\text{adp}}$  largest activations and sets all others to zero. The encoder matrix  $W_{\text{enc}} \in \mathbb{R}^{M \times d}$ , decoder matrix  $W_{\text{dec}} \in \mathbb{R}^{d \times M}$ , and bias vector  $b_{\text{pre}} \in \mathbb{R}^d$  are trainable parameters. The output  $\hat{x}$  is given followed Equation 2.

Therefore, the AdaptiveK SAE eliminates the computational burden of training separate models for each sparsity level to find the optimal trade-off, requiring only a single training run. Additionally, it addresses the feature suppression problem that occurs with L1 penalties while improving performance on context-level tasks by allocating representational capacity proportional to context complexity. Experiments in Section 4 demonstrate that this complexity-driven adaptation achieves better reconstruction without requiring extensive hyperparameter tuning.

### 3.3 AdaptiveK Sparse Autoencoder Training

We employ a three-phase training for AdaptiveK SAE (see Algorithm 1). First, we pretrain the complexity estimation probe as described in Section 3.1.

In the second phase, we freeze the probe parameters and train only the SAE components using:

$$L_{\text{SAE}} = L_{\text{recon}} + \alpha L_{\text{sparsity}} + \beta L_{\text{aux}}, \quad (9)$$

where  $L_{\text{recon}} = \|x - \hat{x}\|_2^2$  is the reconstruction loss,  $L_{\text{sparsity}} = \frac{\|z\|_1}{\|x\|_2}$  is the normalized  $L_1$  penalty with weight  $\alpha = 0.005$ , and  $L_{\text{aux}}$  is the auxiliary loss with weight  $\beta = 1/32$  for reactivating dead features. We set  $\text{base\_k} = 80$ ,  $\text{min\_k} = 20$ , and  $\text{max\_k} = 320$  for the sparsity range.

In the final joint fine-tuning phase, we jointly optimize both components with:

$$L_{\text{joint}} = L_{\text{SAE}} + \gamma(L_{\text{probe}} + \delta L_{\text{deviation}}), \quad (10)$$

where  $\gamma = 0.9$  controls the probe loss weight and  $L_{\text{deviation}} = |w - w^0|_2 + |b - b^0|$  penalizes deviations from pre-trained parameters, initially with  $\delta = 1$ . This penalty prevents the SAE's reconstruction objective from corrupting the probe's complexity mapping. We adaptively adjust  $\delta$  between 0.01 and 0.5, decreasing  $\delta$  when probe loss improves and increasing  $\delta$  when it stagnates.

Our implementation uses a AdaptiveKBuffer that extracts last-token representations from contexts (see Section 3.1.1 for details), reducing memory usage while tracking complexity scores for balanced training.

Adam optimizer [32] is applied with learning rate 1e-3, warm-up over 15 steps, and linear decay starting at 70% of training. More SAE training details will be presented in Appendix B.

---

#### Algorithm 1: AdaptiveK SAE Training

---

**Input:** Activation data  $D = \{x_i\}_{i=1}^N$ , random initialized SAE.

// Phase 1: Complexity probe pretraining

Train linear probe to predict complexity scores from activations

// Phase 2: SAE training with frozen probe

**while not converged do**

    Apply adaptive sparsity constraints based on complexity

    Update SAE parameters using

$L_{\text{SAE}} = L_{\text{recon}} + \alpha L_{\text{sparsity}} + \beta L_{\text{aux}}$

// Phase 3: Joint fine-tuning

**while not converged do**

    Update all parameters using

$L_{\text{joint}} = L_{\text{SAE}} + \gamma(L_{\text{probe}} + \delta L_{\text{deviation}})$

**Output:** Trained AdaptiveK SAE.

---

## 4 Experiments

In this section, we evaluate our AdaptiveK to answer the following research questions (RQs):

- **RQ1:** How does the relationship between text complexity and adaptive k-values manifest across different language model scales?
- **RQ2:** To what extent does our adaptive sparsity mechanism improve reconstruction quality metrics (L2 loss, variance explained, and cosine similarity) compared to fixed-sparsity approaches?
- **RQ3:** How does AdaptiveK SAE's performance on the Pareto frontier balance the trade-off between sparsity and reconstruction fidelity compared to baseline methods?



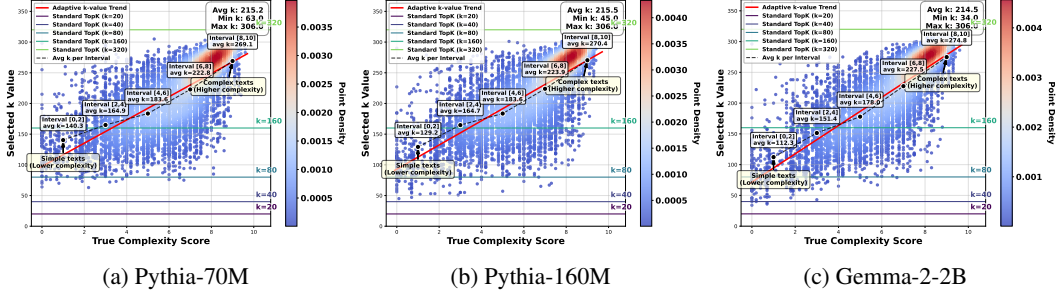


Figure 4: Visualization of Dynamic Feature Allocation by Text Complexity showing the relationship between complexity scores and allocated feature counts (K values). Average K values per complexity interval (connected by red lines) demonstrate that more complex texts receive higher K allocations. This relationship becomes increasingly linear as LLM scale grows. Horizontal lines indicate fixed Standard TopK baselines with K values noted on the right.

#### 4.1 Experimental Settings

We train SAEs on three language models of increasing scale: Pythia-70M, Pythia-160M, and Gemma-2-2B [29, 30], with hidden state dimensions of 512, 768, and 2048 respectively. All trained SAEs have a dictionary size of 16384, i.e., 16k latents. Unlike previous token-level approaches, we operate at the context level, using both training and evaluation data from pile-uncopyrighted [28]. Our training dataset comprises 250,000 contexts, while our test set contains 10,000 contexts, each consisting of 2048 tokens. Following studies on layer-wise functionality [11], we extract activations from layer 3 of Pythia models and layer 12 of Gemma-2-2B. We train on the last token representation of each context, which efficiently captures the accumulated contextual information for complexity-driven sparsity adaptation.

For our experimental evaluation, we compare our AdaptiveK SAE against seven SAE baselines, including: (1) ReLU SAEs [7], the foundational approach using ReLU activation with L1 penalty; (2) refined ReLU\_new SAEs [27]; (3) TopK SAEs [11], which select the K highest activations; (4) BatchTopK SAEs [12], extending TopK across batches; (5) Gated SAEs [10], which decouple feature selection from magnitude estimation; (6) P-anneal SAEs [17], using annealing  $L_p$  norm penalties; and (7) Matryoshka SAEs [16], which train nested dictionaries with increasing capacity.

In addition to the primary metrics discussed in the main text, we utilized a range of metrics from SAE Bench [20], such as ‘Spurious Correlation Removal’ among others, to evaluate AdaptiveK SAE against baseline SAEs. Due to limited space in the main document, further details regarding these evaluations are provided in Appendix C.2. Furthermore, Appendix C.1 explores how the behavior of AdaptiveK SAE differ when it is applied to distinct layers within a single LLM.

#### 4.2 Relationship Between Complexity and k-Values

We plotted the relationship between the true complexity and k-value selection on the test set, calculated the average k-value for each complexity interval, and marked the fixed k-values that TopK would select. As shown in Figure 4, there is an approximately linear relationship between text complexity and allocated k-values, which becomes increasingly evident as model scale increases.

On one hand, examining Figure 3, we observe that both predicted complexity and activated feature count increase with sample complexity. This validates our approach’s effectiveness: complex texts are accurately assessed and mapped to larger k values, activating more features. The results demonstrate the coherence of our complexity-aware sparse autoencoder framework.

On the other hand, considering Figure 5b, 6b and 7b, we observe that while reconstruction errors of TopK SAE gradually decrease as k-values increase, they remain consistently higher than those of AdaptiveK SAE. This demonstrates that AdaptiveK SAE intelligently allocates computational resources by assigning fewer features to simpler texts and more features to complex ones, ultimately achieving superior performance.

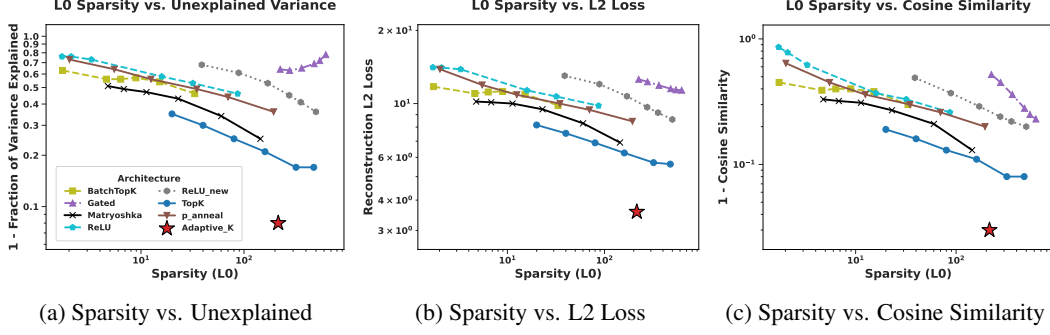


Figure 5: Three Pareto Frontier results on Pythia-70M

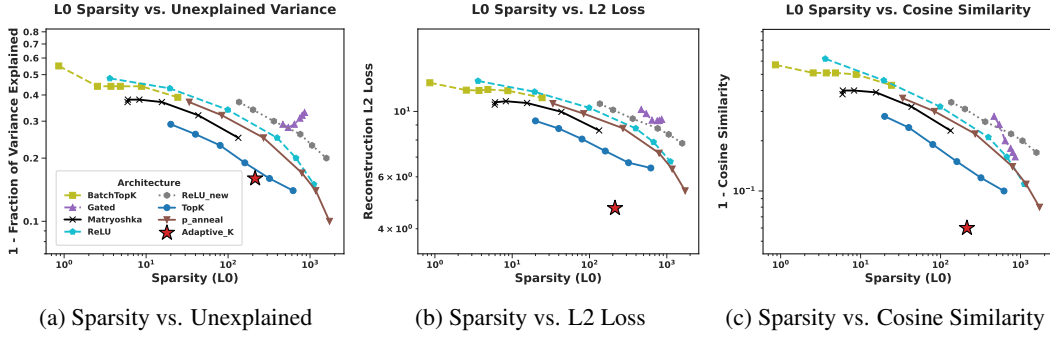


Figure 6: Three Pareto Frontier results on Pythia-160M

### 4.3 Pareto Frontier Results

We evaluated the three different metrics vs. sparsity frontier for benchmark SAEs with different sparsity constraints. All SAEs have a dictionary size of 16384. These three metrics are:

- **Reconstruction L2 Loss:**  $\|x - \hat{x}\|_2^2$  averages the squared Euclidean distance between each reconstruction and its input, the smaller the better.
- **Fraction of Variance Explained:**  $\frac{\text{Var}(x - \hat{x})}{\text{Var}(x)}$  measures how much input variability is captured by the reconstruction. The plots show 1 minus this value (unexplained variance, the smaller the better).
- **Cosine Similarity:**  $\frac{x \cdot \hat{x}}{\|x\|_2 \|\hat{x}\|_2}$  evaluates directional fidelity between original and reconstructed vectors. The plots show 1 minus this value, thus the smaller the better.

Figure 5, 6 and 7 demonstrate that across Pareto Frontier results on different LLMs, AdaptiveK’s reconstruction error remains consistently lower than all other SAE approaches, even as they improve with increased sparsity. For cosine similarity and explained variance, AdaptiveK outperforms at equivalent sparsity levels. While some SAEs match or exceed these metrics at extremely high sparsity (over ten times greater), such cases violate the sparsity-fidelity tradeoff because an infinite-width SAE can theoretically reconstruct perfectly [20]. Thus, our SAE transcends the traditional Pareto Frontier, achieving results unreachable by other SAEs regardless of parameter tuning.

Notably, across all three model scales, AdaptiveK’s reconstructed activations more accurately match the originals in both distance and direction (Figure 5b, 6b, 7b, 5c, 6c, 7c) while explaining a higher proportion of data variance (Figure 5a, 6a, 7a). This consistent cross-model performance demonstrates AdaptiveK’s robustness and generalizability.

## 5 Related Work

### 5.1 Sparse Autoencoders and Improvements

A significant challenge in neural network interpretability is polysemanticity, where units (*e.g.*, neurons) respond to diverse, semantically distinct inputs, complicating functional analysis [6, 1]. The



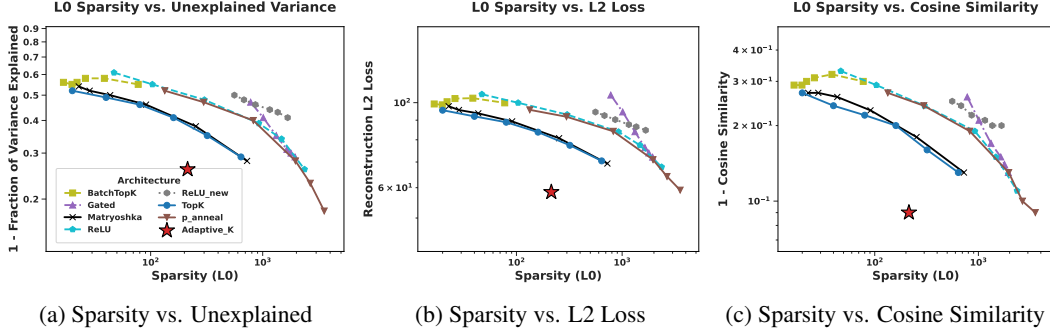


Figure 7: Three Pareto Frontier results on Gemma-2-2B

superposition hypothesis [33] suggests that networks represent more features than available neurons by encoding them as directions in activation space, rather than solely via individual neuron activities. SAEs offer an unsupervised dictionary learning approach to tackle this, decomposing internal network activations (particularly in LLMs) to reveal latent interpretable units [2, 34]. Core to SAEs is an encoder mapping an activation  $x$  to a higher-dimensional sparse representation  $z$ , and a decoder reconstructing  $\hat{x}$  from  $z$ . Goal for SAEs are to isolate monosemantic and composable features, thus offering a more faithful representation of the model’s internal computational state [8, 35].

Following initial SAE proposals [8], research rapidly advanced SAE design. Efforts addressed limitations like L1 penalty-induced shrinkage, leading to Gated SAEs [10]. Alternative sparsity mechanisms emerged, including TopK [11], BatchTopK [12], JumpReLU [13], and ProLU [14]. Architectural innovations like Switch SAEs improved computational scaling [15], while Matryoshka SAEs targeted feature hierarchy and splitting/absorption issues [16]. Optimization objectives were also refined through techniques like P-annealing [17], feature alignment [18], and end-to-end training [19]. While these advancements often optimize proxy metrics like sparsity and fidelity, their alignment with true interpretability remains an active area of evaluation.

## 5.2 Linear Probe in Large Language Models

Linear probes have emerged as a fundamental method for elucidating how LLMs represent complex information within their activation spaces [36, 37, 38]. This approach is grounded in the hypothesis that important high-level concepts are encoded linearly as directions in representational space [22, 39]. A substantial body of research supports the finding that linear probes are more effective than nonlinear probes at aligning model representations with specific behaviors. For instance, Gurnee and Tegmark [24] applied linear probes to Llama-2 models to reveal that LLMs learn linear representations of space and time that are robust to prompting variations, unified across entity types, and encoded by specific neurons within the network. Similarly, Tigges et al. [23] demonstrated that sentiment in language models emerges along specific linear directions in activation space, with a single dimension causally controlling sentiment polarity (positive versus negative) in model outputs through direct interventions. Additionally, concepts such as topic direction [40], political ideology [22], game states [41], truthfulness [42] and safety [43] have also been identified as important features that are linearly encoded within the internal activation spaces of LLMs.

## 6 Conclusions and Future Work

In this paper, we introduce AdaptiveK SAE, demonstrating that dynamically adjusting sparsity based on input complexity significantly improves representation decomposition in LLMs. By establishing that text complexity is linearly encoded in LLM activations, we developed a framework that allocates computational resources proportionally to content complexity, eliminating the need for extensive hyperparameter tuning while consistently outperforming fixed-sparsity baselines across multiple model scales. The experiments on Pythia-70M, Pythia-160M, and Gemma-2-2B confirm that this complexity-driven adaptation achieves better reconstruction fidelity, explained variance, and cosine similarity metrics. In future, we plan to explore applying AdaptiveK SAE to multimodal models, and investigate how our adaptive feature allocation might enhance interpretability for safety alignment.

## References

- [1] Chris Olah, Nick Cammarata, Ludwig Schubert, Gabriel Goh, Michael Petrov, and Shan Carter. Zoom in: An introduction to circuits. *Distill*, 5(3):e00024–001, 2020.
- [2] Javier Ferrando, Gabriele Sarti, Arianna Bisazza, and Marta R Costa-Jussà. A primer on the inner workings of transformer-based language models. *arXiv preprint arXiv:2405.00208*, 2024.
- [3] Chris Olah. Distributed representations: Composition & superposition. *Transformer Circuits Thread*, 27, 2023.
- [4] Sanjeev Arora, Yuanzhi Li, Yingyu Liang, Tengyu Ma, and Andrej Risteski. Linear algebraic structure of word senses, with applications to polysemy. *Transactions of the Association for Computational Linguistics*, 6:483–495, 2018.
- [5] Wes Gurnee, Neel Nanda, Matthew Pauly, Katherine Harvey, Dmitrii Troitskii, and Dimitris Bertsimas. Finding neurons in a haystack: Case studies with sparse probing. *arXiv preprint arXiv:2305.01610*, 2023.
- [6] Nelson Elhage, Tristan Hume, Catherine Olsson, Nicholas Schiefer, Tom Henighan, Shauna Kravec, Zac Hatfield-Dodds, Robert Lasenby, Dawn Drain, Carol Chen, et al. Toy models of superposition. *arXiv preprint arXiv:2209.10652*, 2022.
- [7] Trenton Bricken, Adly Templeton, Joshua Batson, Brian Chen, Adam Jermyn, Tom Conerly, Nick Turner, Cem Anil, Carson Denison, Amanda Askell, et al. Towards monosemanticity: Decomposing language models with dictionary learning. *Transformer Circuits Thread*, 2, 2023.
- [8] Hoagy Cunningham, Aidan Ewart, Logan Riggs, Robert Huben, and Lee Sharkey. Sparse autoencoders find highly interpretable features in language models. *arXiv preprint arXiv:2309.08600*, 2023.
- [9] Adly Templeton, Tom Conerly, Joshua Marcus, Jack Lindsey, Trenton Bricken, Brian Chen, Adam Jermyn, Nicholas L. Turner, Cem Anil, Carson Denison, Amanda Askell, Robert Lasenby, Yifan Wu, Shauna Kravec, Nicholas Schiefer, Tim Maxwell, Nicholas Joseph, Alex Tamkin, Karina Nguyen, Brayden McLean, Josiah E. Burke, Tristan Hume, Shan Carter, Tom Henighan, and Chris Olah. Scaling monosemanticity: Extracting interpretable features from claude 3 sonnet. <https://transformer-circuits.pub/2024/scaling-monosemanticity/index.html>, April 2024. Transformer Circuits Thread. Accessed 2025-05-06.
- [10] Senthoran Rajamanoharan, Arthur Conmy, Lewis Smith, Tom Lieberum, Vikrant Varma, János Kramár, Rohin Shah, and Neel Nanda. Improving dictionary learning with gated sparse autoencoders. *arXiv preprint arXiv:2404.16014*, 2024.
- [11] Leo Gao, Tom Dupré la Tour, Henk Tillman, Gabriel Goh, Rajan Troll, Alec Radford, Ilya Sutskever, Jan Leike, and Jeffrey Wu. Scaling and evaluating sparse autoencoders. *arXiv preprint arXiv:2406.04093*, 2024.
- [12] Bart Bussmann, Patrick Leask, and Neel Nanda. Batchtopk sparse autoencoders. *arXiv preprint arXiv:2412.06410*, 2024.
- [13] Senthoran Rajamanoharan, Tom Lieberum, Nicolas Sonnerat, Arthur Conmy, Vikrant Varma, János Kramár, and Neel Nanda. Jumping ahead: Improving reconstruction fidelity with jumprelu sparse autoencoders. *arXiv preprint arXiv:2407.14435*, 2024.
- [14] Glen M. Taggart. Prolu: A nonlinearity for sparse autoencoders. <https://www.alignmentforum.org/posts/HEpufTdakGTTKgoYF/prolu-a-nonlinearity-for-sparse-autoencoders>, 2024.
- [15] Anish Mudide, Joshua Engels, Eric J Michaud, Max Tegmark, and Christian Schroeder de Witt. Efficient dictionary learning with switch sparse autoencoders. *arXiv preprint arXiv:2410.08201*, 2024.

- [16] Bart Bussmann, Patrick Leask, and Neel Nanda. Learning multi-level features with matryoshka saes, december 19 2024b. In URL <https://www.alignmentforum.org/posts/rKM9b6B2LqwSB5ToN/learning-multi-level-features-with-matryoshka-saes>. *Alignment Forum*, 2024.
- [17] Adam Karvonen, Benjamin Wright, Can Rager, Rico Angell, Jannik Brinkmann, Logan Smith, Claudio Mayrink Verdun, David Bau, and Samuel Marks. Measuring progress in dictionary learning for language model interpretability with board game models. *Advances in Neural Information Processing Systems*, 37:83091–83118, 2024.
- [18] Luke Marks, Alasdair Paren, David Krueger, and Fazl Barez. Enhancing neural network interpretability with feature-aligned sparse autoencoders. *arXiv preprint arXiv:2411.01220*, 2024.
- [19] Dan Braun, Jordan Taylor, Nicholas Goldowsky-Dill, and Lee Sharkey. Identifying functionally important features with end-to-end sparse dictionary learning. *Advances in Neural Information Processing Systems*, 37:107286–107325, 2024.
- [20] Adam Karvonen, Can Rager, Johnny Lin, Curt Tigges, Joseph Bloom, David Chanin, Yeu-Tong Lau, Eoin Farrell, Callum McDougall, Kola Ayonrinde, et al. Saebench: A comprehensive benchmark for sparse autoencoders in language model interpretability. *arXiv preprint arXiv:2503.09532*, 2025.
- [21] Matthew E Peters, Mark Neumann, Luke Zettlemoyer, and Wen-tau Yih. Dissecting contextual word embeddings: Architecture and representation. *arXiv preprint arXiv:1808.08949*, 2018.
- [22] Junsol Kim, James Evans, and Aaron Schein. Linear representations of political perspective emerge in large language models. *arXiv preprint arXiv:2503.02080*, 2025.
- [23] Curt Tigges, Oskar John Hollinsworth, Atticus Geiger, and Neel Nanda. Linear representations of sentiment in large language models. *arXiv preprint arXiv:2310.15154*, 2023.
- [24] Wes Gurnee and Max Tegmark. Language models represent space and time. *arXiv preprint arXiv:2310.02207*, 2023.
- [25] OpenAI. GPT-4.1 Mini - OpenAI API, 2024. URL <https://platform.openai.com/docs/models/gpt-4.1-mini>.
- [26] Samuel Marks, Adam Karvonen, and Aaron Mueller. dictionary\_learning. [https://github.com/saprmaks/dictionary\\_learning](https://github.com/saprmaks/dictionary_learning), 2024.
- [27] Anthropic Interpretability Team. Circuits updates—april 2024. <https://transformer-circuits.pub/2024/april-update/index.html>, April 2024.
- [28] Leo Gao, Stella Biderman, Sid Black, Laurence Golding, Travis Hoppe, Charles Foster, Jason Phang, Horace He, Anish Thite, Noa Nabeshima, et al. The pile: An 800gb dataset of diverse text for language modeling. *arXiv preprint arXiv:2101.00027*, 2020.
- [29] Stella Biderman, Hailey Schoelkopf, Quentin Gregory Anthony, Herbie Bradley, Kyle O’Brien, Eric Hallahan, Mohammad Aflah Khan, Shivanshu Purohit, USVSN Sai Prashanth, Edward Raff, et al. Pythia: A suite for analyzing large language models across training and scaling. In *International Conference on Machine Learning*, pages 2397–2430. PMLR, 2023.
- [30] Gemma Team, Morgane Riviere, Shreya Pathak, Pier Giuseppe Sessa, Cassidy Hardin, Surya Bhupatiraju, Léonard Hussenot, Thomas Mesnard, Bobak Shahriari, Alexandre Ramé, et al. Gemma 2: Improving open language models at a practical size. *arXiv preprint arXiv:2408.00118*, 2024.
- [31] Yonatan Belinkov. Probing classifiers: Promises, shortcomings, and advances. *Computational Linguistics*, 48(1):207–219, 2022.
- [32] Diederik P Kingma and Jimmy Ba. Adam: A method for stochastic optimization. *arXiv preprint arXiv:1412.6980*, 2014.

- [33] Kiho Park, Yo Joong Choe, and Victor Veitch. The linear representation hypothesis and the geometry of large language models. *arXiv preprint arXiv:2311.03658*, 2023.
- [34] Dong Shu, Xuansheng Wu, Haiyan Zhao, Daking Rai, Ziyu Yao, Ninghao Liu, and Mengnan Du. A survey on sparse autoencoders: Interpreting the internal mechanisms of large language models, 2025. URL <https://arxiv.org/abs/2503.05613>.
- [35] Robert Huben, Hoagy Cunningham, Logan Riggs Smith, Aidan Ewart, and Lee Sharkey. Sparse autoencoders find highly interpretable features in language models. In *The Twelfth International Conference on Learning Representations*, 2023.
- [36] Kenneth Li, Oam Patel, Fernanda Viégas, Hanspeter Pfister, and Martin Wattenberg. Inference-time intervention: Eliciting truthful answers from a language model. *Advances in Neural Information Processing Systems*, 36:41451–41530, 2023.
- [37] Dimitri Von Rütte, Sotiris Anagnostidis, Gregor Bachmann, and Thomas Hofmann. A language model’s guide through latent space. *arXiv preprint arXiv:2402.14433*, 2024.
- [38] Tomáš Mikolov, Wen-tau Yih, and Geoffrey Zweig. Linguistic regularities in continuous space word representations. In *Proceedings of the 2013 conference of the north american chapter of the association for computational linguistics: Human language technologies*, pages 746–751, 2013.
- [39] Sheng Liu, Haotian Ye, Lei Xing, and James Zou. In-context vectors: Making in context learning more effective and controllable through latent space steering. URL <https://arxiv.org/abs/2311.06668>, 2024.
- [40] Alexander Matt Turner, Lisa Thiergart, Gavin Leech, David Udell, Juan J Vazquez, Ulisse Mini, and Monte MacDiarmid. Steering language models with activation engineering. *arXiv preprint arXiv:2308.10248*, 2023.
- [41] Neel Nanda, Andrew Lee, and Martin Wattenberg. Emergent linear representations in world models of self-supervised sequence models. *arXiv preprint arXiv:2309.00941*, 2023.
- [42] Samuel Marks and Max Tegmark. The geometry of truth: Emergent linear structure in large language model representations of true/false datasets. *arXiv preprint arXiv:2310.06824*, 2023.
- [43] Andy Ardit, Oscar Obeso, Aaquib Syed, Daniel Paleka, Nina Panickssery, Wes Gurnee, and Neel Nanda. Refusal in language models is mediated by a single direction. *arXiv preprint arXiv:2406.11717*, 2024.

## A Linear Probes Training Details

Our training methodology employs texts from the pile-uncopyrighted corpus, which are processed through a tokenizer and aggregated into contexts of 1024 tokens each. Each context undergoes a comprehensive six-dimensional evaluation by GPT-4.1-mini, resulting in a normalized complexity score between 0 and 10 with one decimal place precision. Our dataset comprises 250,000 training contexts and 10,000 test contexts.

For each context, we extract the activation vector of the final token as the representational vector for that context, with dimensionality matching that of the model's hidden layer. During training, batches of unprocessed activation values are sequentially retrieved from the buffer and marked as processed. When all activations have been utilized, the buffer is replenished and shuffled to introduce stochasticity. This iterative cycle continues until a sufficient quantity of activation samples has been accumulated for effective model training.

Below are some examples with various complexity scores, their predicted complexities by the linear probe, corresponding K-values, and the number of activated latent features through AdaptiveK SAE:

### Sample 1:

True Complexity: 1.2 || Pred Complexity: 3.18 || K value: 95 || Activated Features: 95

```
\u00f4m\u00e9",\n      \u00e9 de commerce",\n      \u00e9 de commerce CFC",\n      \u00e9 de remont\u00e9s m\u00e9caniques\n      AFP",\n      \u00e9 d\u00e9 exploitation AFP",\n      \u00e9 en cuisine AFP",\n      \u00e9 en h\u00e9tellerie AFP",\n      \u00e9 en industrie laiti\u00e8re AFP",\n      \u00e9 en intendance AFP",\n      \u00e9 en intendance AFP",\n      \u00e9 en restauration AFP",\n      \u00e9 en restauration AFP",\n      douane avec dipl\u00f4me f\u00e9d\u00e9ral",\n      \u00e9 en entra\u00eeneur de\n      sport de performance avec brevet f\u00e9d\u00e9ral...
```

### Sample 2:

True Complexity: 3.5 || Pred Complexity: 4.26 || K value: 137 || Activated Features: 137

```
max-age=31536000; includeSubDomains\nx-aspnet-version: [4.0.30319]\n-x-content-type-options: [nosniff]\nx-ms-ratelimit-remaining-subscription\n-resource-requests: ['11998']\nx-powered-by: [ASP.NET]\nstatus: {\n  code: 201, message: Created\n  request: \n  body: null\n  headers: \n  Accept: [application/json]\n  Accept-Encoding: ['gzip, deflate']\n  CommandName: [network dns zone import]\n  Connection: [keep-alive]\n  Content-Type: [application/json; charset=utf-8]...
```

### Sample 3:

True Complexity: 5.2 || Pred Complexity: 5.39 || K value: 187 || Activated Features: 187

```
very much interested in the idea of sanctuary. How do the spirits of these two authors and the respective sanctuaries they sought infuse Tom and Nathan\u2019s interactions? What other giants of American literature have an influence, direct or indirect, on the characters in The Brooklyn Follies?\n\n\u201cYou love life,\u201d says Nathan to Tom, \u201cbut you don\u2019t believe in it. And neither do I.\u201d This statement quickly becomes untrue as both men cast off their inertia. To what extent does action create belief for bo...
```

**Sample 4:**  
**True Complexity: 6.2 || Pred Complexity: 6.05 || K value: 216 || Activated Features: 216**

```
itself implement the\n    // interface because that exposes all the public
methods of that interface at the manager level.\n    private static final
String INTENT_URL_PREFIX = \"intent:\";\n\n    // The animation duration of
a URL being promoted to a tab when triggered by an\n    // intercept
navigation. This is faster than the standard tab promotion animation\n    //
so that it completes before the navigation.\n    private static final long
INTERCEPT_NAVIGATION_PROMOTION_ANIMATION_DURATION_MS = 40;\n\n    ...
```

**Sample 5:**  
**True Complexity: 9.1 || Pred Complexity: 9.19 || K value: 298 || Activated Features: 242**

parameters of the MSSM and to trace back, sector-wise, the sensitivity to initial conditions of the Yukawa couplings and the soft susy breaking parameters. We have established analytically a generic screening of non-universality, in the vicinity of the infrared quasi fixed points. In practice, this property gives the general trend of the behaviour, despite the large number of free parameters, and even when one is not very close to such a quasi fixed point. This shows that non-universality of th...

**Sample 6:**  
**True Complexity: 9.6 || Pred Complexity: 8.91 || K value: 294 || Activated Features: 294**

```
{\{\ensurermath{\mathbbm{R}}\}^d\} \to [0,\infty)$ satisfy for all $d\in \{\mathbbm{N}\}$, $x=(x_1,\ldots,x_d)\in \{\ensurermath{\mathbbm{R}}\}^d$ that $\mathbbm{A}_d(x)=\left(\max\{x_1,0\},\ldots,\max\{x_d,0\}\right)$ and $\|x\|=[\sum_{i=1}^d(x_i)^2]^{1/2}$, let $\mathbbm{H}=\cup_{H\in \{\ensurermath{\mathbbm{N}}\}}\cup_{\{(k_0,k_1,\ldots,k_{H+1})\in \{\ensurermath{\mathbbm{N}}\}^{H+2}\}}\prod_{n=1}^{H+1}\left(\{\ensurermath{\mathbbm{R}}\}^{k_n}\times k_{n-1}\right)\times\ensurermath{\mathbbm{R}}$.
```

## B Additional SAE Training Details

Our SAEs are trained on the residual stream because researchers typically focus on this component when interpreting or steering model behaviors. This alignment ensures the learned representations directly support the most common SAE applications in model analysis and intervention. Our code is available at: <https://anonymous.4open.science/r/adaptiveK-5258>

The training and testing datasets for the AdaptiveK SAE are consistent with those utilized in the linear probe training phase. The overall training process is determined by the current step value, with three distinct phases: step=0 is the pre-training phase, dedicated to probe training; step < total steps×phase ratio involve training the SAE while maintaining frozen probe parameters; step > this threshold initiate the joint fine-tuning phase. The total step count is calculated by dividing the total token count (250,000) by the batch processing capacity (2048 tokens), with phase ratio set at 0.9.

During the third phase, the deviation weight adapts dynamically throughout training. The system maintains records of probe losses from the three most recent steps and calculates the rate of loss change. When rapid loss reduction occurs (change rate exceeding the threshold 0.5), the deviation weight is reduced to 0.8 of its original value; otherwise, it increases to 1.2, with an upper limit of 0.5. A sigmoid function maps predicted complexity scores (0-10) to feature quantity ranges (from min\_k to max\_k, established at 20 to 320), with the sigmoid midpoint corresponding to base\_k (80) and steepness (0.6) controlling the mapping curve’s configuration. This enables the AdaptiveK SAE to dynamically allocate sparsity by assigning fewer features to simpler texts (low complexity) while allocating more features to complex texts (high complexity).

As the AdaptiveK SAE was trained on 250,000 token activations, we employed identical training and testing datasets for training and evaluating baseline SAEs, with their sparsity configurations detailed in Table 2.



Table 2: Sparsity setting of baseline SAEs

SAE	Sparsity	Pythia	Gemma
TopK		20, 40, 80, 160, 320, 640	
Batch TopK	K Value	20, 40, 80, 160, 320, 640	
Matryoshka Batch TopK		20, 40, 80, 160, 320, 640	
Gated		0.6, 0.9, 1.2, 2, 3, 4	2.4, 3.6, 4.8, 8, 12, 16
Relu	Sparsity Penalties	0.6, 0.9, 1.2, 2, 3, 4	2.4, 3.6, 4.8, 8, 12, 16
Relu_new		0.6, 0.9, 1.2, 2, 3, 4	2.4, 3.6, 4.8, 8, 12, 16
P Anneal		0.3, 0.45, 0.6, 1, 1.5, 2	1.2, 1.8, 2.4, 4, 6, 8

## C Additional Experimental Evaluation

### C.1 Analysis of Layers

We trained AdaptiveK SAE on each layer of Pythia-160M and on layers 4, 8, 12, 16, 20, and 24 of the Gemma-2-2B model. A cross-layer comparison of key performance metrics is presented in Table 3 and 4. L2 ratio measures the proportion between the L2 norms of reconstructed and original activations, with values closer to 1 indicating preservation of the original activation magnitude. AdaptiveK exhibits robust performance across all tested layers in both models, with Explained Variance, Cosine Similarity, and L2 Ratio consistently above 0.74, 0.91, and 0.89 respectively. This confirms the algorithm’s generalizability throughout the entire LLM hierarchy.

Table 3: Layer-wise performance in Pythia-160M

Layer	Explained Variance	Cosine Similarity	L2 Ratio
0	0.90	0.96	0.91
1	0.86	0.95	0.91
2	0.85	0.95	0.91
3	0.84	0.94	0.89
4	0.83	0.94	0.89
5	0.85	0.96	0.94
6	0.89	0.96	0.93
7	0.91	0.97	0.95
8	0.91	0.97	0.96
9	0.89	0.96	0.95
10	0.86	0.96	0.95
11	0.89	0.99	0.99

### C.2 Other Evaluation Metrics

In this section, we evaluate the AdaptiveK SAE using five metrics from SAEBench [20]. For the Feature Absorption metric, we directly compare the results of AdaptiveK SAE with those of the baseline SAEs reported in SAEBench, **noting that their training dataset was 2000 times larger than ours**. For the remaining metrics, (Spurious Correlation Removal, Targeted Probe Perturbation, Resolving Attribute-Value Entanglements in Language Models, and Sparse Probing), the AdaptiveK SAE is compared against baseline SAEs trained on an identical amount of training data.

Table 4: Layer-wise performance in Gemma-2-2B

Layer	Explained Variance	Cosine Similarity	L2 Ratio
4	0.81	0.93	0.93
8	0.80	0.93	0.93
12	0.74	0.91	0.92
16	0.77	0.92	0.93
20	0.79	0.93	0.94
24	0.77	0.92	0.93

### C.2.1 Feature Absorption

One of the primary objectives of SAEs is to enhance feature interpretability through sparse activation patterns. However, when concepts exhibit hierarchical relationships, concept A (*e.g.*, red) inherently implies a broader concept B (*e.g.*, color), instead of dedicating separate, clear latents for both A and B, SAEs tend to develop a latent unit representing A and another representing “B except A”. While this approach optimizes sparsity, it significantly compromises interpretability.

Following [20], Feature Absorption is measured using a first-letter classification task. It first establishes a “ground truth” directional vector  $p$ , for each first-letter concept by training linear probes on the base language model’s activations ( $a_{model}$ ). It then identifies a set of “main” SAE latents ( $S_{main}$ ) expected to represent each letter. The core of the measurement involves analyzing individual instances (words). For an instance, if the main latents don’t fully capture the ground truth signal (i.e.,  $\sum_{i \in S_{main}} a_i d_i \cdot p < a_{model} \cdot p$ , where  $a_i$  is latent activation and  $d_i$  its decoder vector), and other “absorbing” latents ( $S_{abs}$ ) that align with  $p$  compensate for this deficit, an absorption fraction is calculated. Let  $P_{main} = \sum_{j \in S_{main}} a_j d_j \cdot p$  be the projection from main features, and  $P_{compensated\_by\_absorbers}$  be projection from the top few absorbing latents that cover the signal portion not captured by  $P_{main}$ . The instance-level absorption fraction  $f_{abs}$  is then:

$$f_{abs} = \frac{P_{compensated\_by\_absorbers}}{P_{compensated\_by\_absorbers} + P_{main}}. \quad (11)$$

This value closer to 0 means less feature absorption. We calculate two metrics: Mean Absorption Fraction per letter is the average of these  $f_{abs}$  values over all relevant instances for that letter. Separately, an instance is marked for full absorption if stricter binary criteria are met: essentially, if main features are inactive and a single, dominant non-main latent (aligned with  $p$ ) overwhelmingly represents the letter’s ground truth signal. The Full Absorption Rate per letter is simply the proportion of relevant instances for that letter which meet these conditions for “full absorption”, indicating how often extreme absorption occurs.

Utilizing this metric, we assessed the performance of our AdaptiveK SAE on layer 3 of Pythia-160M and layer 12 of Gemma-2-2B, as shown in Figure 8 and 9. Notably, when directly benchmarked against SAEs from SAEBench [20] for Gemma-2-2B’s layer 12, AdaptiveK exhibited superior results on both metrics (Figure 10). This outperformance is particularly significant given that our AdaptiveK was trained on only 250,000 tokens, a dataset 2000 times smaller than the 500,000,000 tokens used for the SAEBench models. In AdaptiveK, concepts are correctly allocated to their intended primary latents rather than being dispersed across unrelated variables. Cases where concepts are entirely misrepresented in non-primary latents are notably rare. This demonstrates AdaptiveK’s exceptional effectiveness in maintaining conceptual integrity and preventing feature fragmentation.

### C.2.2 Spurious Correlation Removal (SCR)

Spurious Correlation Removal evaluates an SAE’s ability to disentangle distinct concepts by measuring how effectively it can remove spurious correlations from classifiers. Likewise, utilizing method from SAEBench [20], we first generated biased datasets containing spurious correlations (*e.g.*, professor+male and nurse+female from the Bias in Bios dataset). A linear classifier is then trained on this biased dataset, learning to rely on both the target concept (profession) and the spurious concept (gender). To evaluate an SAE, the method identifies latents most strongly associated with

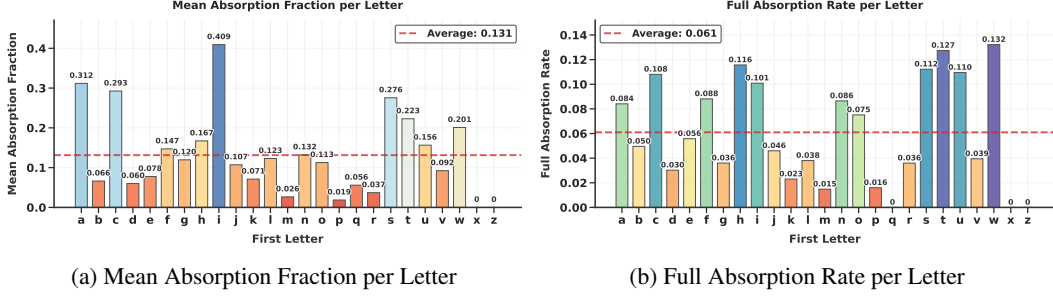


Figure 8: Letter Absorption Results on Pythia-160M

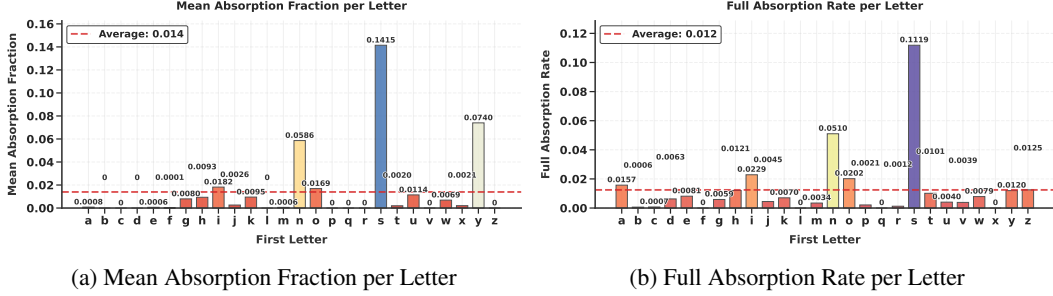


Figure 9: Letter Absorption Results on Gemma-2-2B

the spurious concept (gender) through probe attribution scores. These identified latents are then zero-ablated, creating a modified classifier. The final SCR score is normalized as:

$$\text{SCR Score} = \frac{A_{\text{abl}} - A_{\text{base}}}{A_{\text{oracle}} - A_{\text{base}}}, \quad (12)$$

where  $A_{\text{abl}}$  is accuracy after ablation,  $A_{\text{base}}$  is baseline accuracy, and  $A_{\text{oracle}}$  is the accuracy of a classifier trained directly on the desired concept. Higher SCR scores indicate better concept disentanglement, suggesting the SAE effectively isolates distinct concepts into separate latents.

The results of comparing the AdaptiveK SAE trained on Pythia-160M layer 3 against other baseline SAEs, where all SAEs were trained using 250,000 tokens, are depicted in Figure 11. SCR Top10 and SCR Top20 refer to the SCR scores when ablating the top 10 and top 20 latents respectively that are most associated with the spurious concept. AdaptiveK shows dramatically higher SCR scores in both settings, directly indicating its superior concept disentanglement, with clearer separation between concepts like gender and profession. Additionally, it produces latent representations where concepts are more cleanly isolated in specific latents, enabling more effective debiasing of classifiers.

### C.2.3 Targeted Probe Perturbation (TPP)

Unlike SCR which works with binary correlated labels, TPP extends SCR to multiclass settings. For each class  $i$  in a dataset with  $m$  classes, TPP identifies the most relevant latents  $L_i$  for that class and trains linear classifiers  $C_j$  for each class  $j$  with accuracy  $A_j$ . Then, it creates modified classifiers  $C_{i,j}$  by ablating latents  $L_i$ , with accuracy  $A_{i,j}$ . We can calculate TPP Score as:

$$\text{TPP Score} = \text{mean}_{i=j}(A_{i,j} - A_j) - \text{mean}_{i \neq j}(A_{i,j} - A_j). \quad (13)$$

This formula captures the difference between within-class effects (when  $i = j$ ) and cross-class effects (when  $i \neq j$ ). A high TPP score indicates good disentanglement, ablating latents for class  $i$  primarily affects only class  $i$ 's accuracy while leaving other class accuracies unchanged. This shows concepts are encoded in separate, non-overlapping latent dimensions. In the same way, TPP Top10 and TPP Top20 refer to the TPP scores when ablating the top 10 and top 20 most relevant latents for each class, respectively.

As shown in Figure 12, AdaptiveK outperforms most SAEs, showing that ablating latents identified for one class primarily affects only that class's probe accuracy. This precise targeting indicates

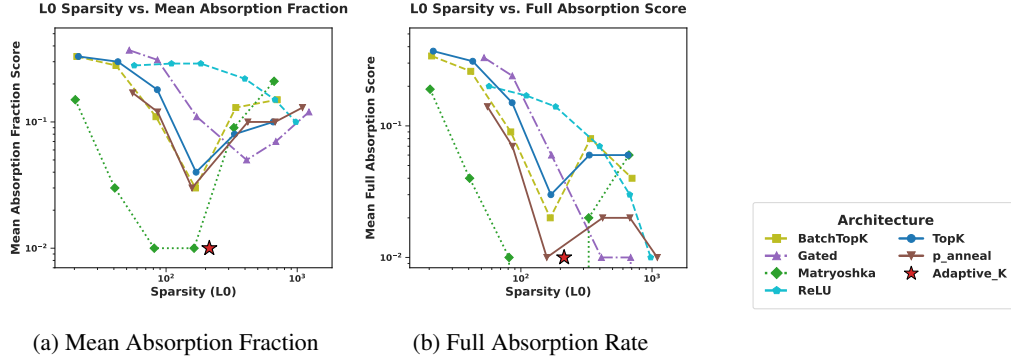


Figure 10: Two Feature Absorption metrics across different SAEs on Gemma-2-2B Layer 12

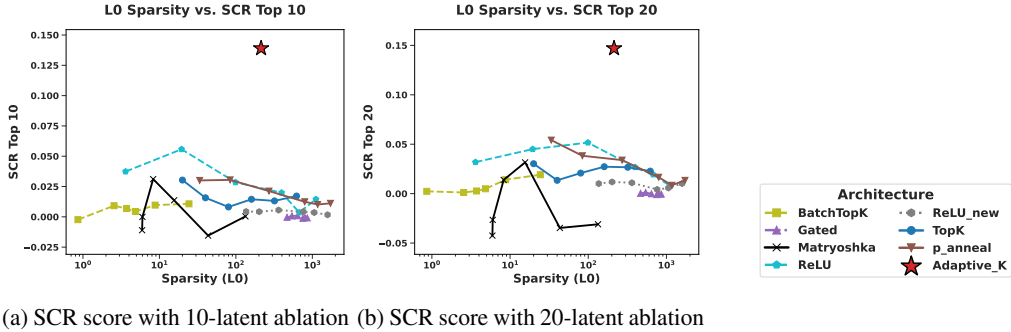


Figure 11: SCR scores across two intervention settings on Pythia-160M Layer 3

AdaptiveK organizes its latent space with clearer conceptual boundaries. Combined with its SCR results in Figure 11, AdaptiveK creates a more structurally organized latent space with minimal concept overlap. While Matryoshka Batch TopK performs well on TPP, AdaptiveK’s consistent high performance across both TPP and SCR metrics demonstrates its representation efficiently separates both binary concepts and multiclass classes. This dual strength in disentanglement makes it particularly suited for interpretability tasks requiring precise concept isolation and targeted.

#### C.2.4 Resolving Attribute-Value Entanglements in Language Models (RAVEL)

RAVEL directly measures a key application of interpretability, which is the practical utility of an SAE for targeted knowledge editing. It tests whether interventions on specific latents can modify one attribute of an entity while preserving other attributes. The evaluation focuses on whether an SAE can help a language model make targeted factual modifications, for example, changing Paris’s country from France to Japan while correctly maintaining that the language spoken there is still French (rather than incorrectly switching to Japanese). The evaluation begins by collecting high-confidence entity-attribute predictions across five diverse categories (cities, Nobel laureates, physical objects, etc.). For each entity, RAVEL identifies which latents most strongly encode specific attributes using trained probes. It then tests what happens when these latents are manipulated - can the model be made to believe Paris is in Japan while still knowing French is spoken there? This capability is measured through two complementary metrics: the cause score (how effectively the intervention changes the target attribute) and the isolation score (how well other attributes remain unaffected). These are averaged into a final disentanglement score. Higher scores indicate better attribute separation in the SAE’s latent space, showing it has successfully disentangled different factual properties into distinct latent dimensions that can be independently manipulated.

In the disentanglement score (Figure 13a), AdaptiveK achieves 0.62, substantially higher than contemporary architectures like TopK and Matryoshka at comparable sparsity levels. For the cause score (Figure 13b), AdaptiveK reaches 0.6, roughly double the effectiveness of other SAEs at similar sparsity. This indicates AdaptiveK is exceptionally good at identifying and modifying the specific latents that control target attributes (like a city’s country). The isolation score (Figure 13c) shows

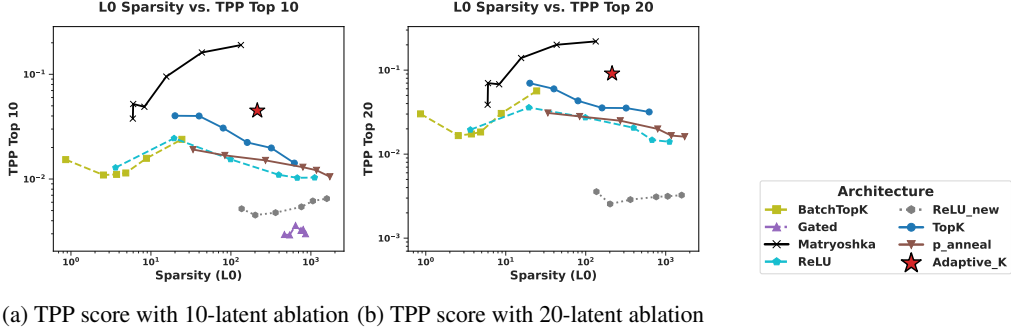


Figure 12: TPP scores across two intervention settings on Pythia-160M Layer 3

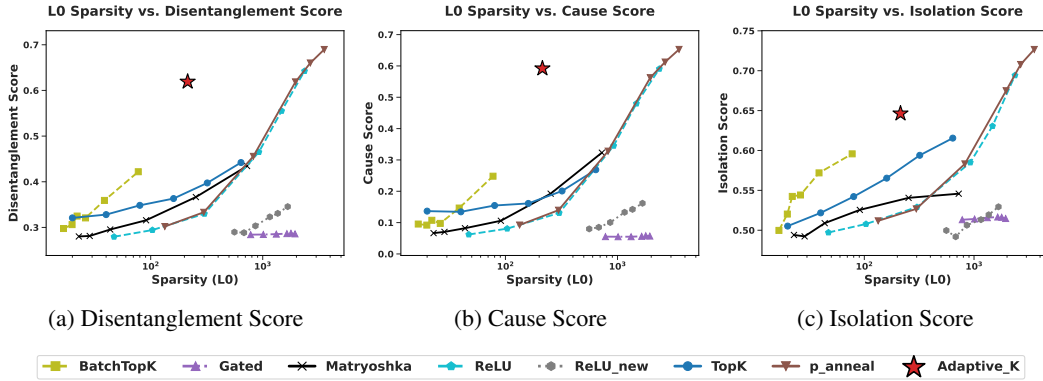


Figure 13: Three RAVEL results on Gemma-2-2B Layer 12

AdaptiveK at 0.65, demonstrating it maintains unrelated attributes more effectively than others. While P Anneal and some other SAEs eventually reach similar or higher disentanglement scores, they require much higher sparsity levels ( $L0 > 1000$ ) to do so, making them less practical for interpretability work that benefits from more compact representations. Combined with the earlier SCR and TPP results, these RAVEL findings confirm that AdaptiveK creates a latent space with exceptionally clean separation between different concepts and attributes, enabling more precise and controlled interventions on language model knowledge.

### C.2.5 Sparse Probing

Unlike other metrics that focus on concept separation, Sparse Probing evaluates an SAE’s ability to organize meaningful semantic features by measuring how effectively it concentrates concept-specific information in individual latents. The method applies the SAE to encode texts from five diverse datasets covering profession classification (Bias in Bios), product categorization and sentiment analysis (Amazon Reviews), language identification (Europarl), programming language detection (GitHub), and news topic categorization (AG News). For each of the 35 binary classification tasks, the evaluation first identifies which latents show the greatest activation difference between positive and negative examples. A logistic regression probe is then trained using only these selected latents (ranging from just the single most relevant latent to the top 5), with performance measured on 1,000 held-out test examples. The key insight is that if the SAE has effectively organized information, even a small number of latents (the top-K) should contain sufficient information to perform specific classification tasks.

Metric “Full Activations Accuracy” represents classification performance when using all SAE activations, establishing an upper bound. Metrics “Top-K Accuracy” (where K is 1, 2, or 5) measure performance when restricting the probe to only the K most relevant latents for each task. First, we measure information retention rate (SAE Full Activations Accuracy / LLM Full Activations Accuracy), which quantifies how well each SAE preserves the original model’s information when using all

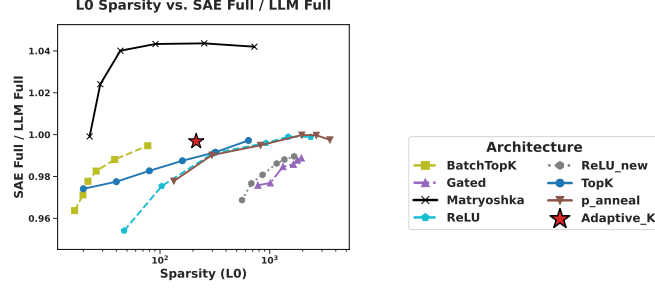


Figure 14: SAE Full Accuracy / LLM Full Accuracy on Gemma-2-2B Layer 12

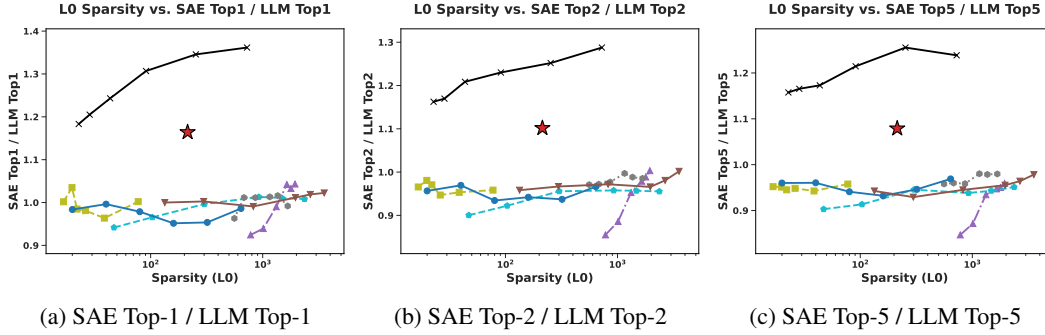


Figure 15: SAE Top-K / LLM Top-K on Gemma-2-2B Layer 12

reconstructed activations. As shown in Figure 14, AdaptiveK’s retention ratio of approximately 0.997 demonstrates near-perfect preservation of the original model’s information. While Matryoshka’s slightly higher ratio ( $>1$ ) suggests beneficial feature reorganization or denoising during reconstruction, such enhancement represents a supplementary advantage rather than a necessity.

Second, we examine relative feature concentration (SAE Top-K / LLM Top-K) across three granularities ( $K=1,2,5$ ) as illustrated in Figure 15. These metrics reveal how efficiently each architecture concentrates concept-specific information in its most relevant latents compared to the base model. The SAE Top-K/LLM Top-K ratios for AdaptiveK consistently exceed 1. Though marginally below Matryoshka, these values convincingly demonstrate AdaptiveK’s superior ability to concentrate concept-relevant information in fewer latent dimensions than the original model requires, indicating more efficient latent space organization.

Finally, we assess information concentration efficiency (SAE Top-K / SAE Full) in Figure 16, which measures how much of an SAE’s total information is captured in its  $K$  most relevant latents. AdaptiveK captures approximately 82% of its complete representation using just its most relevant single latent variable, surpassing most other SAE architectures and demonstrating exceptional information compression.

Collectively, these metrics establish AdaptiveK’s balanced excellence: it maintains original model information (retention rate), concentrates more concept-relevant information in fewer dimensions than the original model (relative feature concentration), and achieves a highly organized internal representation that localizes most information in a minimal number of latents (information concentration efficiency).

## D Limitations and Broader Impacts

### D.1 Limitations

Due to the cost constraints associated with API annotation, our study utilized a significantly smaller training dataset compared to the 500,000,000 tokens employed in SAE Bench. Specifically, we



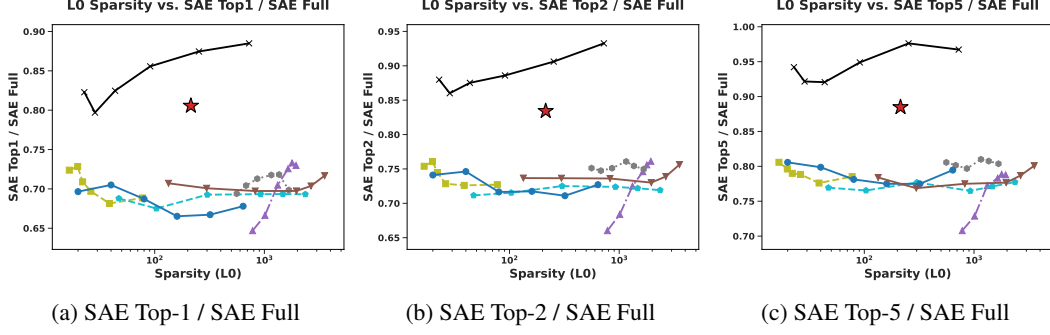


Figure 16: SAE Top-K / SAE Full on Gemma-2-2B Layer 12

trained on 250,000 contexts, extracting the activation value of the final token from each context as its representational vector. Despite this substantial reduction in training data volume, our AdaptiveK SAE achieved impressive performance across most evaluation metrics, with some results even surpassing the baseline SAEs reported in SAE Bench. This remarkable efficiency demonstrates the considerable potential of our approach. Rather than relying exclusively on extensive training data, we have introduced a novel SAE training algorithm that fundamentally rethinks sparsity allocation.

## D.2 Broader Impacts

Our AdaptiveK Sparse Autoencoder offers significant broader impacts across multiple domains. By dynamically allocating representational capacity based on input complexity, it enhances computational efficiency through optimized resource utilization, potentially reducing energy consumption in large-scale AI systems. This adaptive approach simultaneously improves model interpretability by establishing clear correlations between complexity metrics and feature activation patterns, providing researchers with new insights into representation learning mechanisms.

## Prompt for Scoring Context Complexity

### Detailed Evaluation Dimensions

1. Lexical Complexity (*Weight: 20%*): Evaluate the vocabulary sophistication level using the following criteria
  - Word Frequency: Proportion of uncommon words (not in the 5000 most frequent words)
  - Word Length: Average syllable count and character length of words
  - Lexical Diversity: Type-token ratio (unique words divided by total words)
  - Technical Terminology: Presence of specialized or domain-specific vocabulary
  - Lexical Density: Ratio of content words (nouns, verbs, adjectives, adverbs) to function words (pronouns, prepositions, articles, etc.)
2. Syntactic Complexity (*Weight: 20%*): Analyze sentence-structure complexity using these metrics
  - Sentence Length: Average number of words per sentence
  - Clause Density: Number of clauses per sentence
  - Subordination: Frequency and depth of subordinate clauses
  - Passive Voice: Proportion of sentences in passive voice
  - Syntactic Variety: Diversity of sentence structures
  - Embedding Depth: How deeply clauses are nested within one another
3. Conceptual Density (*Weight: 25%*): Assess the density and abstraction level of ideas presented
  - Concept Count: Number of distinct concepts, ideas, or arguments introduced
  - Concept Abstraction: Level of concreteness vs. abstraction of concepts
  - Conceptual Networks: Complexity of relationships between concepts
  - Information Density: Amount of information conveyed per paragraph
  - Theoretical Complexity: Depth of theoretical constructs presented
4. Domain Specificity (*Weight: 15%*): Evaluate how much specialized domain knowledge is required
  - Background Knowledge: Prerequisite knowledge assumed by the text
  - Domain Vocabulary: Concentration of field-specific terminology
  - Conceptual Familiarity: How familiar concepts would be to general readers
  - Specialized References: References to domain-specific methods, theories, or figures
  - Audience Specificity: How targeted the text is to specialists vs. general readers
5. Logical Structure (*Weight: 10%*): Analyze the complexity of reasoning patterns
  - Argument Structure: Complexity of argumentative or explanatory structure
  - Logical Operations: Presence of conditional, causal, comparative reasoning
  - Inference Requirements: Extent to which the reader must infer rather than being told explicitly
  - Logical Connections: Clarity and complexity of connections between ideas
  - Reasoning Chains: Length and complexity of logical chains
6. Contextual Dependencies (*Weight: 10%*): Assess how much the text relies on external context
  - Intertextual References: References to other texts or knowledge sources
  - Cultural Knowledge: Required cultural or historical background
  - Implicit Information: Amount of information that remains unstated yet necessary
  - Presuppositions: Assumptions the text makes about reader knowledge
  - Discourse Context: Degree to which meaning depends on broader discourse context

### Text to Evaluate

{text}

### Required Output Format

Only return a JSON object with the following structure:

```
{
  "lexical_complexity": {
    "score": <0-10 number>
  },
  "syntactic_complexity": {
    "score": <0-10 number>
  },
  "conceptual_density": {
    "score": <0-10 number>
  },
  "domain_specificity": {
    "score": <0-10 number>
  },
  "logical_structure": {
    "score": <0-10 number>
  },
  "contextual_dependencies": {
    "score": <0-10 number>
  },
  "final_weighted_score":
    <calculated final score as decimal>,
  "normalized_complexity_score":
    <rounded to one decimal place, e.g. 4.5>
}
```